

# Detection of buried landmines using a *casi* hyperspectral imager

John E. McFee<sup>a</sup> and Herb T. Ripley<sup>b</sup>

<sup>a</sup>Threat Detection Group, Defence Research Establishment Suffield,  
Box 4000, Medicine Hat, AB, Canada, T1A 8K6

<sup>b</sup>Ripley and Associates,  
7 Betty Jane Court, Dartmouth, NS, Canada, B2W 5Z9

## ABSTRACT

Experiments were conducted to estimate the probability of detection (Pd) and false alarm rate (FAR) for detection of buried mines using a *casi* hyperspectral imager scanned from a personnel lift. Surrogate mines and blocks of explosive were buried under various vegetative covers and bare soil using standard mine laying methods. Images were obtained at various times from 1 2/3 to 15 1/2 months after burial. Mines under short and medium length vegetation and bare soil were detectable by calculating the linear correlation coefficient or fractional composition, derived from orthogonal subspace projection, for each pixel of the image. Pd for surrogates decreased with increasing vegetation length and appeared to vary somewhat with environmental conditions. Short vegetation gave better detection results than bare soil which gave better results than medium length vegetation. Pd was typically in the range of 55 to 94% and FAR varied from about 0.17 to 0.52 m<sup>-2</sup>. There were insufficient data to assess the relative importance of stress due to explosive vapour leaching into the soil compared to stress induced by soil disturbance.

**Keywords:** Mine detection, Hyperspectral imaging, Reflectance, Linear correlation coefficient, Fractional composition

## 1. INTRODUCTION

The feasibility of identifying surface-laid mines from an airborne platform using visible wavelength hyperspectral imaging has previously been demonstrated.<sup>1,2</sup> A *casi* imager was used to obtain hyperspectral radiometric images of mines and backgrounds which were converted to reflectance images using information from an incident light sensor (ILS). Both low altitude (~6 m) and high altitude (~300 m) imagery have been obtained. A variety of surrogate and replica mines have been distinguished from a variety of background types with high probabilities of detection and low false alarm rates for widely varying illumination conditions caused by diurnal and seasonal variations, sky conditions and sun angles. The imager has even been able to detect mines partially obscured by vegetation. As an example, on the left side of Fig. 1 is a three colour image (printed in grey scale) of a region containing surface-laid surrogate mines taken at an altitude of ~300 m from a helicopter. The surrogates are green squares with widths approximately equal to the pixel width (~50 cm) and are invisible on the full colour image. On the right is the single band image of the same region processed from a 16 band *casi* image using a method described in Ref. 2. Each white blob is a mine. The probability of detection of individual mines for this image is 100% and the false alarm rate is 0.

Buried mines cannot be detected directly in the visible band, due to the high absorption of radiation by the soil and vegetation cover but may be indirectly detected by observation of differences in reflectance spectra between compact regions over top of mines and regions of background materials due to

1. disturbed versus undisturbed vegetation and surface soil,
2. vegetative stress due to mine implantation even if the surface is apparently undisturbed,
3. vegetative stress due to explosive vapours originating either from leaks in the mine case or from residue contaminating the case.

---

Other author information: (Send correspondence to J.E.M.)

J.E.M.: Email: John.McFee@dres.dnd.ca; Telephone: 403-544-4739; Fax: 403-544-4704; Supported by the Research and Development Branch, Department of National Defence, Canada, under Project Number 2HB11.

H.T.R.: Email: hripley@fox.nstn.ca; Telephone: 902-462-3242; Fax: 902-462-6674

In a previous preliminary study,<sup>3</sup> surrogate mines were detected 1 2/3 months after burial under vegetative cover by analysis of hyperspectral images from a *casi* mounted in a horizontally scanned personnel lift. The results verified the second of the above mechanisms, but due to the scope of that study, the first and third were not tested. Further, probabilities of detection and false alarm rates could not be estimated and duration of the effect could not be monitored beyond 2 months post-burial.

To resolve these issues, further studies were conducted starting one year after the original study. An improved ground truthing method was implemented to allow probabilities of detection and false alarm rates to be estimated. Hyperspectral images of mines buried from the first study plus images from mines buried 1 year after the first study were obtained over a period of three months. Mines were buried in vegetative cover and bare soil. To estimate the effect of the third mechanism, explosive blocks were buried in an identical manner to the surrogates.

The images were processed using bands and techniques selected to detect changes in vegetation and nonvegetative substrates.

## 2. PROCEDURE

To study soil disturbance and inclusion effects on vegetation, the mine burial patches that were established in the previous study were again used. Surrogate mines had originally been buried on August 8 1995 in 7 patches of land at Canadian Forces Base Gagetown, New Brunswick, Canada. Each patch had a different vegetative cover or bare soil cover and all were in exposed areas having no natural shade. Two cylindrical surrogate mine types were used. The large antitank (AT) surrogate was 25 cm in diameter and 8.7 cm thick, while the smaller one, simulating an antipersonnel (AP) mine, was 10.5 cm in diameter and 4.6 cm thick. Both were made of solid plastic and closely matched the overall thermal properties of real mines. Each patch, surrounded by a wire fence, contained three rows of two mines each. A row consisted of an AT surrogate beside an AP surrogate, separated by roughly 1 m. Rows were spaced roughly 1 m apart and the order of AP/AT was alternated for each new row. Mines and patches are described more fully in Ref. 3. All mines were buried using standard mine laying practice. The mines in vegetative cover patches were emplaced by making a slit in the earth with a shovel, lifting the sod flap, removing sufficient dirt so that the flap would be flush with the ground surface afterwards, emplacing the mine and replacing the flap. For bare soil patches, the ground was too crumbly to use the previous procedure. Instead, a hole was dug deep enough so that the mine could be emplaced and covered with dirt, leaving the surface flat and smooth. Excess dirt was removed. All mines were buried at tactical depths, approximately 8 to 15 cm between ground surface and mine top. Immediately after the burial process, none of the vegetation covered mine burial sites could be detected with the naked eye. The bare soil covered mine sites were initially, under close inspection, faintly but distinctly visible, but after a few days in the sun they became indistinguishable from the surrounding soil.

Reconnaissance on July 28 1996 revealed that the wire and fencing used to demarcate the patches had been removed and thus, all mines had to be relocated. The general vicinities of the patches were obtained from map references and minelaying notes from the previous year. The specific location of each mine was then determined by manual probing using Canadian Forces prodders. This was done slowly and painstakingly so as to minimally disturb the surface and subsurface. A red disk was centered over each mine after locating it. Next reference pins were stuck in the ground at the four corners of each patch. A clear plastic sheet was stretched tight over the whole patch and staked down to the reference pins. A fluorescent green blob of paint was then sprayed on the plastic immediately over the center of each disk. This sheet could then be used as a ground truth sheet. Plastic sheet and disks were removed and reserved for later use. One of the previous sites (patch I) had been buried under 30 to 60 cm of soil by a road grader during the winter. Since the patch was unusable, the mines were dug up and reburied on July 29, 1996 using an identical procedure as above in a new grassy site (patch O). All patches were demarcated with survey twine stretched taut around the reference pins, in the hope that it was less conspicuous than the fencing and hence less likely to be stolen.

To study the effect of buried explosive vapour or particulates on vegetative stress, explosives were buried on July 29, 1996 under medium height grass cover (patch P). Three burial sites, each separated by roughly 1 m, were situated in the ammunition storage facility at CFB Gagetown. Explosives were buried between 8 and 10 cm deep, according to the method described above. The first site contained 3 sticks of C4 plastic explosives, totalling 1.70 Kg, with their original plastic wrappers removed. The second site contained an identical 3 sticks of explosives, with their wrappers intact. The third site was an empty hole, dug in the same manner as the two previous holes, but refilled

with dirt. The first hole was intended to introduce a large amount of explosive vapour into the soil. The amount was deliberately much larger than that provided by a typical mine, since it was desired to separate the effect due to disturbing the site from that due to the explosive vapour. The second site was a control for disturbed soil when an inclusion is present. Minimal explosive vapour or particulates would leach into the soil, since the hermetically sealed plastic wrap provides an excellent barrier. The third site was a control for soil disturbance under the vegetation with no inclusion. The composition and history of all test patches are summarized Fig. 2.

Images of the patches were obtained using a DRES-owned compact airborne spectrographic imager (*casi*), manufactured by ITRES Research Ltd., Calgary, Canada. The instrument is a hyperspectral visible (VIS) and near infrared (NIR) waveband (400-1000 nm) imager which uses a diffraction grating to spread the slit image across a two dimensional charge coupled device (CCD), producing a spectral vector of up to 288 elements for each pixel of the image.<sup>4</sup> The instrument is shown in Fig. 3.

Images were obtained in spatial mode using a 15 band bandset (Fig. 4) which provides uniform coverage across the full visible spectrum, together with good coverage of the major spectral absorption and reflection features of vegetation. Extra coverage is provided along the red edge and bands are available to characterize the near IR shoulder to facilitate modelling the sigmoidal-shaped red edge. The bandset is very similar to the bandset used in the previous study,<sup>3</sup> except that the new bandset has omitted a redundant band centered near 708 nm. Images were also collected in hyperspectral mode to provide finer waveband coverage across the entire visible band at the expense of decreased swath width and/or scan speed. One mode provided 48 bands, each between 6.1 and 6.3 nm wide, which uniformly spanned the visible band from 407.2 nm to 955.0 nm. A second mode provided 72 bands each between 4.2 and 4.3 nm wide which uniformly spanned the same wavelength range as the 48 band set.

The *casi* is a pushbroom scanner which requires a smooth linear forward motion to produce a two dimensional spectral image. The horizontal linear motion was obtained by mounting the instrument in a JHG 45HA articulated arm personnel lift. The lift had a jointed arm, one part of which could be extended some height above the ground and an attached part which could be extended or retracted horizontally from that elevated point.

Data collection dates are shown in Fig. 2. For the 1996 study, the sensor head was scanned over the target areas at a nominal height of 6.10 m and covered an along-track length of approximately 2.5 m (dictated by the maximum extent of the lift arm). The across-track width was 3.9 m for 512 pixels and proportionately less for fewer across track pixels. Scan times took approximately 30 seconds, corresponding to a scan velocity of about 10 cm/sec. Along-track spatial resolution was a function of scan speed and integration time. The latter varied for different bandsets and illumination conditions, giving along-track pixel lengths between  $\sim 0.8$  cm and 1.3 cm. The height and instrument optics dictated the across-track resolution and gave a pixel width  $\sim 1.4$  cm.

To obtain images, the personnel lift was driven into position near a patch and adjusted such that its arm when scanned horizontally would cover as many of the mine sites in the patch as possible. (Due to constraints in positioning the lift, it was not always possible to include all mine sites in a scan.) Two spatial mode images were obtained by scanning the lift arm over the patch at a uniform horizontal speed. Next the ground truth sheet was stretched tight over the patch and staked down to the same reference pins that had been used when the sheet was first marked. The lift arm was then scanned to obtain an image of the ground truth sheet. The *casi* was then reconfigured to hyperspectral mode and a second image of the ground truth sheet was taken. The sheet was then removed and two more images of the patch were taken. Not including initial setup of the personnel lift, between 8 and 10 minutes were required to collect all images from one patch. The procedure was then repeated for the remaining patches.

### 3. ANALYSIS

#### 3.1. Reflectance image extraction

Raw image data units were corrected for electronic offset, dark current, scattered light and frame shift smear and then converted to spectral radiance units using ITRES calibration software. The incident light sensor (ILS) is a skyward-looking cosine diffuser which provides a signal at the instrument entrance slit which is proportional to the down welling solar radiation. The ILS values for a particular image line are stored in the last row of CCD pixels for the line. The ILS values, together with a knowledge of the sun angle when the image was acquired, can be used to convert the radiance image into a reflectance image. For detection of surface-laid mine-like targets, the reflectance spectrum in the 500 to 680 nm band, calculated in this manner, has been shown to be independent of diurnal and seasonal illumination variations to within an offset and scale factor.<sup>1</sup>

### 3.2. Spectral classification methods

It is well known<sup>5</sup> that a number of regions of the visible reflectance spectrum can display marked differences between senescent and nonsenescent vegetation. In addition, surface disturbance might also alter the reflectance spectra of vegetation and soils, making mine sites detectable. Thus, comparison of spectra from known mine positions or known backgrounds with unknown image spectra on a pixel by pixel basis might reveal the presence of a mine. To this end, average spectral vectors were extracted from the regions immediately above the buried mines for each image. Regions over mines were chosen to be square with sides between 20 and 30 cm. This was typically less than the extent of the bare soil disturbances or sod flaps and ensured that the spectra were a representative average over the area immediately above the mine which could be expected to be affected by the mine presence. Average spectral vectors of various regions not near the mines, representing different background materials, were also extracted. These reference spectra were put into libraries for use with the spectral classifiers.

Two classifiers were used in this study, both of which have been successful in detecting surface-laid and buried mine surrogates in *casi* images.<sup>1-3</sup> Other common classifiers were not suitable for this study. The shift in the red edge of the reflectance spectrum is a classification method frequently used in remote sensing to distinguish between senescent and nonsenescent vegetation.<sup>6</sup> The reduced bandwidth required for measurement of the red edge shift would give it an advantage over the chosen classifiers. Unfortunately, our previous study using spatial mode data showed that mines were not detectable using red edge shift measurements, although this has not been confirmed for the more finely sampled hyperspectral mode data.

The linear correlation coefficient (LCC) is a measure of similarity between an unknown spectral reflectance vector and a reference vector, computed for each pixel on an image. It can be shown<sup>1</sup> that the LCC is insensitive to the spectral scale and offset factors exhibited by the reflectance spectra of experiments such as these. End member analysis and spectral angle mapping (the latter being a special case of the LCC) do not have this property. The range of LCC values in this study was somewhat compressed, with most values lying between roughly 0.25 and 0.7. A variety of contrast stretching and enhancement techniques were applied to the LCC images. These included a power law stretch<sup>2</sup> and linear, Gaussian, histogram equalization and square root stretches available from the ENVI spectral image processing package.<sup>7</sup>

LCC classification relies on the spatial resolution being sufficiently high so that individual pixels contain essentially only one material. Because of the multitude of different materials observed in a small area for most of the images obtained, it was felt that alternate classification techniques should be attempted. We have used Orthogonal Subspace Projection (OSP) in previous studies to detect subpixel extent surface-laid mine surrogates.<sup>2</sup> OSP assumes a linear mixing model in which the spectral reflectance vector at a given spatial position is the weighted sum of the reflectance vectors of the materials (end members) found within the pixel, with weights given by the area fractional composition of the materials. The measured spectral vector is projected onto a subspace which is orthogonal to that which is spanned by the vectors of the background materials.<sup>8</sup> A matrix approximating the latter can be estimated from the covariance matrix of the image under the assumption that the fraction of the image corresponding to target areas is small. This optimally nulls the composite background material vectors in a least squares sense. The fractional composition (FC) of the target material for each pixel can then be estimated by a set of matrix operations<sup>2</sup> and an image of FC values formed.

## 4. RESULTS AND DISCUSSION

### 4.1. General observations

During the July 1996 preinspection, it was observed that the majority of mine locations were invisible to the naked eye, even when viewed only a few centimeters from the mine location. The exceptions were 3 mine locations each on patches E and G which could be seen by close inspection. The vegetation over these locations appeared less healthy than the surrounding vegetation and in one location on patch G, a hive of hornets had established itself under the sod flap. It should be noted that none of the locations had been visible to the eye when initially buried one year before or when images had been obtained 1 2/3 months and 2 1/2 months after burial. The single AT surrogate buried in tall ferns (patch M) was never located due to a lack of precise ground truthing and the substantial difficulty in probing large areas of tall vegetation. Since it was unobservable in 1995 due to the tall vegetation, it was felt that it would be likely unobservable by the *casi* after a year. The patch was thus declared terminated, even though

the surrogate was not recovered. The relaid mine sites in bare soil patches A,C were initially slightly darker than background, but after a few days in sun they became indistinguishable from the background soil.

A summary of dates and types of images collected is presented in Fig. 2. A minor snowfall occurred two days before the November 5 1996 data collection. Although the snow had melted by the time of the experiment, the soft ground prevented the personnel lift from accessing patches A,C and O. In place of *casi* images, colour photographs were taken of these patches in an attempt to identify any mine sites by broadband differences from background. Some of the mine sites in the bare soil patches (3 in A, 3 in C) had depressions over them due to soil settling, partly due to the recent freeze/thaw, and had collected ice in the depressions which made them visible to the eye. This agreed with observations of last year's bare soil experiments in which mines were initially invisible to the eye and then 1 2/3 months later were visible due to depressions in the soil. Conditions for data collection were good, with generally clear skies at the beginning leading to some cloud development throughout the day. Ground cover was quite wet due to the melted snow and illumination levels were very good. For the November 25 1996 experiment, the air was cold and dry and the ground was dry and frozen. Conditions for data collection were good, with high uniform overcast skies and good illumination levels.

All of the August 14 1996 *casi* images and the November 25 1996 images of patch P have not been processed by the time of writing due to technical difficulties, but will be analysed at a later date.

## 4.2. Classification results

For each patch, LCC images were obtained using a number of mine spectral reference vectors and background reference vectors and probabilities of detection (Pd) and false alarm rates (FAR) were estimated. An example LCC image of a short vegetation patch is shown in Fig. 5. The image is derived from a 48 band hyperspectral mode image of patch G taken on November 25 1996. The reference spectral vector used was averaged from a background region away from the mines. The image has been contrast enhanced using an interactive linear stretch from ENVI. Centers of squares coincide with the ground truthed centers of the 4 mines in the field of view. All 4 mine sites are visible as dark blobs against the background.

To estimate Pd and FAR, a hit was first defined to be a compact region (blob) in the contrast enhanced LCC image, roughly equal in area to that of an AT mine ( $\sim 500 \text{ cm}^2$ ). The blob had to be visibly distinct from the rest of the image. If the hit center occurred within 1 AT mine diameter of the mine center, it was declared a detection, otherwise a false alarm. Pd was defined as the number of detections divided by the number of mines in the field of view (FOV) of the image. FAR was defined as the number of false alarms divided by the area of the FOV. Pd and FAR entries in Figs. 6 to 8 are averages of the values for the various mine or background reference vectors used for each entry (rounded down for Pd and up for FAR). In spite of care being taken to not form a bias, it must be cautioned that this was not a blind analysis. Patches E and K were designed to simulate "machine-laid" mines. The burial procedure was exactly the same as Section 2, except that instead of an individual slit being made for each mine, one slit the length of each row was made for each row of mines. It was thought that this long linear disturbance might mask the blob-like disturbance due to individual mines. Hence, for patches E and K, detection was also attempted by looking in the LCC image for distinct linear features of high or low LCC, oriented in the same direction as the mine layer slits and of length roughly equal to the row lengths. Detection of such a feature, if it covered all mines in a row, was deemed to constitute detection of all mines in the row.

The results of classification of the November 5 1996 images are presented in Fig. 6. Hyperspectral mode results are not shown since they were similar to the spatial mode results. Results of spatial mode images are derived from LCC images while results of the photographic images are based on inspection of the photographs. Among the surrogate mine patches, Pd ranged from 33 to 100% with FAR from 0.10 to 0.51  $\text{m}^{-2}$ . AT surrogates were more detectable than AP surrogates, presumably due to the increased area of disturbance required to bury the former. Detection was easier in patches E and G than in patch K. This was in agreement with previous observations<sup>3</sup> which indicated that Pd decreased as length of vegetation increased. This may be due to the increased resistance to stress of the longer vegetation or motion of stems and leaves by wind action which can significantly blur the image. In the 1995 experiments, it was observed that wind gusts sometimes made plant leaves extend up to 30 cm from the location of the roots, contaminating spectral features of the surrounding regions. Probability of detection was the same for blob detection and linear feature detection for patch E, since the blobs were distinct and stood out against the linear disturbances. In patch K, however, detection of blobs was significantly poorer than detection of linear features, since

the blobs were only faintly visible. The difference between patches E and K is likely due to the difference in vegetation length. For the only recently buried vegetative cover patches, Pd was moderate in patch O, and slightly higher in patch P. Since mines in short grass were detected last year after 1 2/3 months burial, the likely explanation for the moderate detection rate is the medium length of vegetation over patches O and P. This is further supported by the fact that Pd for patches O and P are similar to that of patch K which also has medium length vegetation. Two out of three burial sites in patch P were detected. The blank hole was not detected, the unwrapped explosive site was slightly visible and the wrapped explosive site had the best contrast. This suggests that detectability increases with the presence of a foreign body, but that explosive vapour is not a factor, at least after 2 months burial. Due to the small sample size, however, this observation should be treated as a preliminary one. Although detection rates for the photographic images are comparable to the hyperspectral images, no clear conclusions can be drawn since the age of mine burial and the materials covering the photographed patches do not correspond to those of the *casi* imaged patches.

The results of LCC classification of the November 25 1996 hyperspectral mode images are presented in Fig. 7. Spatial mode results are not shown since they were similar to the hyperspectral mode results. Results are generally the same as those of November 5, but slight differences do exist. Overall Pd for patches A,C and O were slightly lower than for November 5, while overall Pd for patches E,G and K were essentially the same for the two dates. FAR was comparable for the two dates. These differences may be partly due to the uncertainty in declaring individual hits, statistical fluctuations for small numbers and the difference in ground conditions between the two days.

Due to time constraints, FC images were computed for only a select few of the November 25 1996 hyperspectral mode images. It was found that the LCC gave slightly better results than the OSP analysis. There are some likely reasons for this, which are hinted at by the fact that FC values were occasionally less than 0. This makes no physical sense, but is allowed by the analysis. Negative values are an indicator that the reference spectra do not adequately model the target spectra or that the background spectra are not adequately modelled. The OSP analysis determines the background spectral subspace by assuming that the image as a whole contains little contribution from target spectral vectors (mines). For these experiments, 2-3% of the image area could be targets and so it is not completely certain how well the assumption holds. In addition, only minimal optimization of the analysis to model the background was allowed.

## 5. CONCLUSIONS

Recent experiments have confirmed our preliminary results that buried surrogate mines can be detected in short to medium length vegetative cover by linear correlation coefficient or orthogonal subspace projection analysis of reflectance images from a *casi* VIS/NIR hyperspectral imager. The mines were not detectable immediately after burial, but were detectable as early as 1 2/3 months afterwards and continued to be detectable more than 15 1/2 months after burial. For vegetative cover, detection is due to a small but measurable differences in the reflectance spectra of vegetation likely caused by stress due to the burial process. For bare soil cover, detection is partly due to colour differences between disturbed and undisturbed soil. Initially, these differences are provided by the difference in colour between the surface soil and upturned subsurface soil. Later it may be caused by differential moisture absorption in the disturbed and undisturbed areas. Detection is also achieved by looking for circular depressions formed above the mines due to soil settling. These may be detected by looking for compact regions with crescent-shaped shadows on one side and brighter reflectance crescents on the other side.

Preliminary Pd and FAR have been estimated for different cover types. Values for November 1996 are summarized in Fig. 8, where the best of linear feature or blob feature detection results have been used for each patch and date combination and then results have been totalled for each cover type. Pd for surrogates decreased with increasing vegetation length. Short vegetation gave better detection results than bare soil which gave better results than medium length vegetation. Pd were typically in the range of 55 to 94% and FAR varied from about 0.17 to 0.52  $m^{-2}$ . Although slight differences in results were observed between wet and dry ground conditions, no clear trends were observed. Only a limited comparison of LCC and FC images was allowed, with LCC performing slightly better than OSP analysis. OSP analysis was not optimized, however, and more study is needed.

There were no significant differences in classification between using 48 or 72 element spectral vectors which uniformly spanned the VIS/NIR spectrum versus 15 element vectors placed at strategic wavelengths. Previous research had shown that analysis of a coarsely sampled narrow portion of the spectrum, at the red edge, did not

give good results. This suggests that the spatial mode vectors, although not necessarily optimized for discriminatory power, are a good compromise to a many element full spectral band vector.

There were insufficient data at this time to assess the relative importance of stress due to explosive vapour leaching into the soil compared to stress induced by soil disturbance. The site containing buried explosive blocks will be monitored again after a one year delay. Blocks may also be buried under grass cover that is shorter than that currently being used.

Improvement of Pd and FAR will be necessary if hyperspectral image detection of buried mines is to be practical. Obvious areas to investigate are to improve classification algorithms and optimize the spectral vectors. This will involve a systematic pattern classification study, emphasizing discriminant analysis and feature analysis. One less obvious approach is to reinvestigate red edge shift analysis. Although shown to be inferior to the currently used spectral vectors, the previous red edge analysis used a very limited number of coarsely spaced elements to define the edge. The available hyperspectral mode data could provide many more elements in the red edge region, allowing much better modelling. This may prove superior to using the full hyperspectral vector. Some of the false alarms are due to variation in shadows caused by differences in sun angle from one measurement time to another. Modelling may allow some of these to be identified as shadow areas. Once this is done, it may be possible to eliminate them by masking and/or removing the very low reflectances common to all spectral elements. Alternatively, a gain factor might be applied to recover the true reflectance values. The optimum time of day and season and environmental conditions for buried mine detection must still be determined, since they may impact dramatically on Pd and FAR. Lastly, hyperspectral imaging experiments in the short wave and long wave infrared bands are also planned to compare results to the VIS/NIR band.

## 6. ACKNOWLEDGMENTS

We wish to thank CWO Ken Walker of the T & E Section, CFB Gagetown, for his efforts in coordinating and carrying out the experiments. We also thank Cpl. D. Boey of Range Control, CFB Gagetown, for his skill in operating the personnel lift and Cpl. Boey, WO Gary Sweet and M.Cpl Vanexan for their efforts in the initial reconnaissance, mine location and reburying.

## REFERENCES

1. J.E.McFee, S.Achal, and C.Anger, "Scatterable mine detection using a *casi*," in *Proceedings of the First International Airborne Remote Sensing Conference*, pp. I587–I598, September 1994.
2. S.Achal, J.McFee, and C.Anger, "Identification of surface-laid mines by classification of compact airborne spectrographic imager (*casi*) reflectance spectra," in *Detection Technologies for Mines and Mine-like Targets*, A.C.Dubey, I.Cindrich, J. Ralston, and K.Rigano, eds., *Proc. SPIE* **2496**, pp. 324–335, 1995.
3. J.McFee, H.Ripley, R.Buxton, and A.Thriscutt, "Preliminary study of detection of buried landmines using a programmable hyperspectral imager," in *Detection and Remediation Technologies for Mines and Mine-like Targets*, A.C.Dubey, R.L.Barnard, C.J.Lowe, and J.E.McFee, eds., *Proc. SPIE* **2765**, pp. 476–488, 1996.
4. C.Anger, S.Mah, and S.Babey, "Technological enhancements to the Compact Airborne Spectrographic Imager (*casi*)," in *Proceedings of the First International Airborne Remote Sensing Conference*, pp. II205–II213, 1994.
5. E.Knipling, "Leaf reflectance and image formation on colour infrared film," in *Remote Sensing in Ecology*, P.L.Johnson, ed., pp. 17–29, University of Georgia Press, Athens, GA, 1969.
6. C.Banninger, "Fluorescence line imager (FLI) measured red edge shifts in metal-stressed Norway spruce forest and their relationship to canopy biochemical and morphological changes," in *Imaging Spectroscopy of the Terrestrial Environment*, *Proc. SPIE* **1298**, pp. 234–243, 1990.
7. Research Systems Inc., Boulder, CO, *ENVI Users Guide Version 2.5*, June 1996.
8. J.C.Harsanyi and C.I.Chang, "Hyperspectral image classification and dimensionality reduction: an orthogonal subspace projection approach," *IEEE Transactions on GeoScience and Remote Sensing* **32**, pp. 779–785, 1994.



**Figure 1.** Airborne *casi* image of a field of surface-laid mine surrogates. Left image is a conventional 3 colour image (printed in grey scale) of the area. Mines widths are roughly equal to a pixel width and the mines are invisible on the full colour image. On the right is the processed *casi* image of the same region. Each white blob is a mine.

Buried Mine Patch Description					First Study			Second Study			
Patch Label	Cover	Vegetation Length	Targets		08/08/95	28/09/95	19/10/95	29/07/96	14/08/96	05/11/96	25/11/96
			Type	Number							
A	bare soil	-	surrogates	3 AT,3 AP	E,I	I	I	R	I	P	I
C	bare soil	-	surrogates	3 AT,3 AP	E,I	I	I	R	I	P	I
E	grass	short	surrogates	3 AT,3 AP	E,I	I	I		I	I	I
G	grass	short	surrogates	3 AT,3 AP	E,I	I	I		I	I	I
I	blueberries	medium	surrogates	3 AT,3 AP	E,I	I	I	T			
K	blueberries	medium	surrogates	3 AT,3 AP	E,I	I	I		I	I	I
M	ferns	long	surrogates	3 AT,3 AP	E,I	I	I	T			
O	grass	medium	surrogates	3 AT,3 AP				E	I	P	I
P	grass	medium	C4 explosive	2 x 1.7 Kg				E	I	I	I

E = Established    R = Re-established    T = Terminated  
I = CASI images obtained    P = Photographic images obtained

**Figure 2.** Description of burial patches used in the 1995 and 1996 studies.





**Figure 3.** *casi* hyperspectral imager. At left from top to bottom are the monitor, control unit and power supply. At right rear is the sensor head.

Spatial Bandset for Buried Mine Detection					
Band Number	Band Center (nm)	Band Width (nm)	Band Number	Band Center (nm)	Band Width (nm)
1	418.9	23.2	9	695.9	10.6
2	446.6	19.6	10	737.0	12.6
3	487.5	12.4	11	746.6	8.8
4	514.5	18.0	12	757.1	6.8
5	548.3	14.2	13	777.2	12.6
6	584.0	18.0	14	816.6	10.6
7	624.7	16.2	15	862.8	10.8
8	667.4	10.6			

**Figure 4.** The spatial mode bandset used in the buried mine detection experiments.

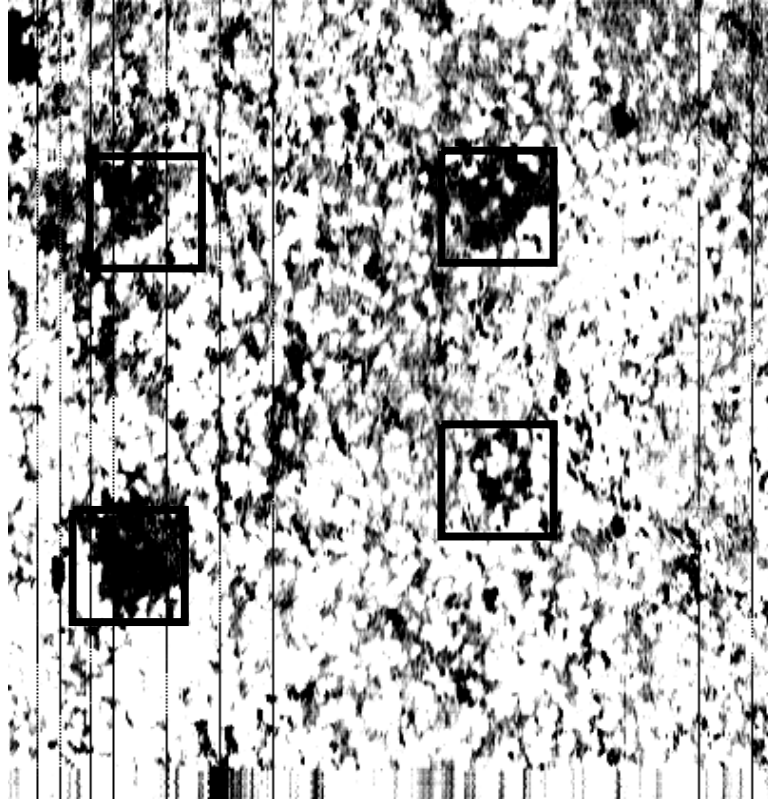


**Figure 5.** LCC image derived from 48 band hyperspectral mode image of patch G taken on November 25 1996. Reference spectral vector used was averaged from a background region away from the mines. Centers of squares coincide with the ground truthed centers of the 4 mines in the field of view.

Detection Rates November 5 1996												
Patch Label	Image <sup>a</sup> Mode	Ref. <sup>b</sup> Vector	Number of Targets Detected						False Alarms			
			AT		AP		Total		#	Area (m <sup>2</sup> )	#/m <sup>2</sup>	
			#	%	#	%	#	%				
A	P	-	3/3	100	2/3	67	5/6	83	1	9.75	0.10	
C	P	-	3/3	100	2/3	67	5/6	83	2	9.75	0.21	
E	S	M	2/2	100	2/2	100	4/4	100	1	9.75	0.10	
		B	2/2	100	2/2	100	4/4	100	1		0.10	
		M	- <sup>d</sup>	-	-	-	4/4	100	1		0.10	
		B	- <sup>d</sup>	-	-	-	4/4	100	1		0.10	
G	S	M	3/3	100	2/3	67	5/6	83	2	9.75	0.21	
		B	3/3	100	2/3	67	5/6	83	2		0.21	
K	S	M	2/3	67	0/3	0	2/6	33	5	9.75	0.51	
		B	2/3	67	0/3	0	2/6	33	5		0.51	
		M	- <sup>c</sup>	-	-	-	4/6	67	5		0.51	
		B	- <sup>c</sup>	-	-	-	4/6	67	5		0.51	
O	P	-	2/3	67	1/3	33	3/6	50	2	9.75	0.21	
P	S	M	-	-	-	-	2/3	67	5	9.75	0.51	
		B	-	-	-	-	2/3	67	5		0.51	

<sup>a</sup> S = Spatial    P = Photographic    <sup>b</sup> M = Mine    B = Background

<sup>c</sup> Detected by looking for linear features : cannot distinguish AT/AP

**Figure 6.** Results of analysis of November 5, 1996 images. Hyperspectral mode results are not shown but are similar to spatial mode results. Detection was based on looking for compact blobs except as noted.

Hyperspectral Mode LCC Detection Rates November 25 1996										
Patch Label	Ref. <sup>a</sup> Vector	Number of Targets Detected						False Alarms		
		AT		AP		Total		#	Area (m <sup>2</sup> )	#/m <sup>2</sup>
		#	%	#	%	#	%			
A	M	0/2	0	2/2	100	2/4	50	1	7.69	0.13
	B	2/2	100	0/2	0	2/4	50	7		
C	M	3/3	100	0/3	0	3/6	50	2	7.69	0.26
	B	3/3	100	2/3	67	5/6	83	1		
E	M	2/2	100	2/2	100	4/4	100	2	7.69	0.26
	B	2/2	100	2/2	100	4/4	100	2		
	M	- <sup>b</sup>	-	-	-	4/4	100	0		
	B	- <sup>b</sup>	-	-	-	4/4	100	0		
G	M	2/2	100	1/2	50	3/4	75	2	7.69	0.26
	B	2/2	100	2/2	100	4/4	100	1		
K	M	1/3	33	1/2	50	2/5	40	5	7.69	0.51
	B	1/3	33	1/2	50	2/5	40	5		
	M	- <sup>b</sup>	-	-	-	3/5	60	5		
	B	- <sup>b</sup>	-	-	-	3/5	60	5		
O	M	1/3	33	1/3	33	2/6	33	1	7.69	0.13
	B	1/3	33	1/3	33	2/6	33	2		

<sup>a</sup> M = Mine    B = Background

<sup>b</sup> Detected by looking for linear features : cannot distinguish AT/AP

**Figure 7.** Results of LCC analysis of November 25, 1996 hyperspectral mode images. Spatial mode results are not shown but are similar to hyperspectral mode results. Detection was based on looking for compact blobs except as noted.

Spatial Mode LCC Detection Rates November 1996 Using Background Reference Vectors					
Cover Type	Number of Targets Detected		False Alarms		
	#	%	#	Area (m <sup>2</sup> )	#/m <sup>2</sup>
Bare Soil	7/10	70	8	15.38	0.52
Short Vegetation	17/18	94	6	34.88	0.17
Medium Vegetation	11/20	55	12	34.88	0.34

**Figure 8.** Results of LCC analysis of November 1996 images using background reference vectors. Best of linear feature or blob feature detection results are taken from each patch and date combination to form the results shown.